

Quantum Monte Carlo Calculations of Neutron- α Scattering

Kenneth M. Nollett, Steven C. Pieper, and R. B. Wiringa

Physics Division, Argonne National Laboratory, Argonne, Illinois 60439, USA

J. Carlson and G. M. Hale

Theoretical Division, Los Alamos National Laboratory, Los Alamos, New Mexico 87545, USA

(Received 8 December 2006; published 12 July 2007)

We describe a new method to treat low-energy scattering problems in few-nucleon systems, and we apply it to the five-body case of neutron-alpha scattering. The method allows precise calculations of low-lying resonances and their widths. We find that a good three-nucleon interaction is crucial to obtain an accurate description of neutron-alpha scattering.

DOI: [10.1103/PhysRevLett.99.022502](https://doi.org/10.1103/PhysRevLett.99.022502)

PACS numbers: 21.60.Ka, 25.10.+s, 21.45.+v, 27.10.+h

There has been significant progress recently in understanding the ground and low-lying excited states of light nuclei through microscopic calculations with realistic two- and three-nucleon interactions [1–3]. These studies have highlighted the importance of including a three-nucleon interaction to obtain correct overall binding of the p -shell nuclei [1], the ordering of states in $^{10,11,12}\text{B}$ [3], and the stability of neutron-rich nuclei [4]. Modern calculations have been very successful in reproducing a large number of the experimentally observed nuclear levels up to mass 12.

A wealth of additional experimental information is available in the form of low-energy scattering and reaction data. Very narrow low-energy resonances have been treated in the above calculations as if they were bound states. Nonresonant scattering and broad resonances have been mostly neglected. The error introduced by the pseudo-bound treatment of narrow resonances is not known quantitatively; no unambiguous energy can be obtained for broad resonances, and no widths are predicted. Methods to treat scattering and resonance states as such will form the foundation for a quantitative, microscopic theory of low-energy nuclear reactions on light nuclei. Such a theory would be useful to astrophysics, because experimental determinations of crucial reaction rates are often difficult or impossible.

A few quantum Monte Carlo (QMC) calculations have been made for multinucleon scattering with true scattering boundary conditions [5–7]. In this Letter we review the method previously used for scattering, present a significantly improved method, and use it to study low-energy neutron-alpha scattering as a five-body problem. We evaluate the two low-lying p -wave resonances with $J^\pi = 3/2^-$ and $1/2^-$, respectively, as well as low-energy nonresonant s -wave ($1/2^+$) scattering.

In each case, we calculate the phase shift as a function of energy for the Argonne v_{18} (AV18) two-nucleon potential [8] alone, and with either the Urbana IX (UIX) model [9] or Illinois-2 (IL2) model [4] three-nucleon potential added. We find significant differences in the calculated phase shifts: the AV18 and AV18 + UIX models produce too

little splitting of the $3/2^-$ and $1/2^-$ states, while AV18 + IL2 reproduces their energies and widths very well. All three models match the low-energy s -wave cross sections. The results demonstrate that experimental phase shifts can be reproduced using realistic interactions with simple modifications to the computational method used for bound states. They also suggest that scattering calculations could provide sensitive constraints on models of the three-nucleon interaction.

In general it is very difficult to treat quantum scattering problems with more than a very few constituents. Often there are many initial or final states, and it is not yet possible to discretize the Schrödinger equation and solve directly for the scattering states. Correct treatment of the boundary conditions for more than two outgoing constituents is also complicated.

For low-energy scattering, though, there are often only a few two-cluster channels open. For one open channel of total angular momentum J and orbital angular momentum L , the wave function at large separation r of clusters with internal wave functions Φ_{c1} and Φ_{c2} will behave as

$$\Psi \propto \frac{1}{kr} \{ \Phi_{c1} \Phi_{c2} Y_L \}_{JJ} [\cos \delta_{JL} F_L(kr) + \sin \delta_{JL} G_L(kr)], \quad (1)$$

where δ_{JL} is the phase shift, $k = \sqrt{2\mu E/\hbar^2}$, E is the scattering energy in the c.m. frame, μ is the reduced mass, F_L and G_L are, respectively, regular and irregular real solutions of the Schrödinger equation with zero nuclear potential, Y_L are spherical harmonics, and $\{ \cdots \}_{JJ}$ denotes angular momentum coupling.

Previous QMC calculations of scattering converted the problem to an eigenvalue problem by imposing a boundary condition $\Psi(r = R_0) = 0$ at a surface radius R_0 beyond the range of the nuclear interaction, and then solving for the energy within this nodal surface [5,10]. Equation (1) then gives $\tan \delta_{JL} = -F_L(kR_0)/G_L(kR_0)$. Finding E as a function of R_0 is equivalent to determining $\delta_{JL}(E)$.

The nodal boundary condition requires different R_0 for different scattering energies. Energies near threshold re-

quire very large R_0 , which can cause numerical difficulties, e.g., Monte Carlo errors that grow as the square root of the sampled volume. It is preferable instead to impose a logarithmic derivative γ on the wave function along the direction $\hat{\mathbf{n}}$ normal to the $r = R_0$ surface:

$$\hat{\mathbf{n}} \cdot \nabla_{\mathbf{r}} \Psi = \gamma \Psi, \quad \text{at } r = R_0. \quad (2)$$

Equation (1) then gives δ_{JL} from E , R_0 , and γ . We can fix R_0 at the minimum necessary and vary γ to produce scattering states of varying E .

We compute nuclear energies by using two QMC methods as successive approximations. The variational Monte Carlo (VMC) method uses a trial wave function $\Psi_T(J^\pi; T)$ with variational parameters that are adjusted to minimize the energy expectation value; Monte Carlo techniques are used to evaluate the integrals over particle position. The method and the form of Ψ_T are described in detail in Refs. [1, 11]. VMC calculations of n - α scattering using a nodal Ψ_T were first made in the 1980s [6]. In the present work, correlations inside Ψ_T (the ϕ_p^{LS} of Ref. [11]) are constrained so that it goes to the form Eq. (1) at large r and satisfies Eq. (2).

Green's function Monte Carlo (GFMC) calculations take Ψ_T and evolve it in imaginary time, τ , to produce $\Psi(\tau) = \exp[-(H - E_0)\tau]\Psi_T$. For large τ , $\Psi(\tau \rightarrow \infty) \propto \Psi_0$, the lowest state with the specified quantum numbers. The propagation time is divided into many small steps of length $\Delta\tau$, for which the exponential can be accurately evaluated, and $\Psi(\tau)$ is computed by iterating the Green's function,

$$G(\mathbf{R}', \mathbf{R}; \Delta\tau) = \langle \mathbf{R}' | \exp[-(H - E_0)\Delta\tau] | \mathbf{R} \rangle, \quad (3)$$

acting on samples of Ψ_T . Here $\mathbf{R} = (\mathbf{r}_1, \mathbf{r}_2, \dots, \mathbf{r}_A)$ is the spatial configuration of the nucleons; although G is an operator, we suppress its spin-isospin labels for simplicity. The nuclear GFMC method is described in Ref. [2]. We include in Eq. (3) all terms of H except those quadratic in orbital angular momentum, which are treated perturbatively. GFMC calculations with the nodal condition at R_0 have been performed for n - α scattering [7] and also for some atomic and condensed-matter problems [12, 13].

In this work, we restrict the GFMC simulation to cluster separations less than R_0 by rejecting Monte Carlo steps that go outside the boundary. The wave function in the restricted volume is the small- r part of a scattering wave function that fills all space, with an energy specified implicitly by the boundary condition. The contributions to $\Psi(\tau)$ at the $(n + 1)$ th $\Delta\tau$ step come from inside and outside the $r < R_0$ region:

$$\begin{aligned} \Psi_{n+1}(\mathbf{R}') &= \int_{|\mathbf{r}| < R_0} d\mathbf{R}_{c1} d\mathbf{R}_{c2} d\mathbf{r} G(\mathbf{R}', \mathbf{R}; \Delta\tau) \Psi_n(\mathbf{R}) \\ &+ \int_{|\mathbf{r}_e| > R_0} d\mathbf{R}_{c1} d\mathbf{R}_{c2} d\mathbf{r}_e G(\mathbf{R}', \mathbf{R}; \Delta\tau) \Psi_n(\mathbf{R}). \end{aligned} \quad (4)$$

Here \mathbf{R} is written in terms of both internal cluster coordinates \mathbf{R}_{c1} and \mathbf{R}_{c2} , and the cluster-cluster separations \mathbf{r}

and \mathbf{r}_e , which, respectively, are contained inside, or extend outside, of the boundary R_0 .

The contribution of the outer region is mapped to an integral over the interior region by a change of variables, $\mathbf{r} = (R_0/r_e)^2 \mathbf{r}_e$ with $r_e = |\mathbf{r}_e|$, in the second term of Eq. (4). A wave function sample at the point \mathbf{R}' is then the sum of one contribution from the previous point \mathbf{R} and one from an ‘‘image point’’ at \mathbf{R}_e , located outside the $r = R_0$ boundary:

$$\begin{aligned} \Psi_{n+1}(\mathbf{R}') &= \int_{|\mathbf{r}| < R_0} d\mathbf{R}_{c1} d\mathbf{R}_{c2} d\mathbf{r} G(\mathbf{R}', \mathbf{R}; \Delta\tau) \\ &\times \left[\Psi_n(\mathbf{R}) + \frac{G(\mathbf{R}', \mathbf{R}_e; \Delta\tau)}{G(\mathbf{R}', \mathbf{R}; \Delta\tau)} \left(\frac{r_e}{r}\right)^3 \Psi_n(\mathbf{R}_e) \right]. \end{aligned} \quad (5)$$

Because $G(\mathbf{R}', \mathbf{R}; \Delta\tau)$ has short range, the $\Psi_n(\mathbf{R}_e)$ can be obtained by linear extrapolation,

$$\Psi_n(\mathbf{R}_e) \approx [1 + \gamma(\mathbf{R}_e - \mathbf{R}) \cdot \hat{\mathbf{n}}] \Psi_n(\mathbf{R}), \quad (6)$$

or by fixing the energy and extrapolating with Eq. (1). The GFMC simulation considers each partition of the nucleons into clusters with separation \mathbf{r} . If the resulting $|\mathbf{r} - \mathbf{r}_e| < 1$ fm, the image contribution is used; otherwise the short range of G makes it insignificant.

This method has several advantages over the nodal boundary condition. Fixing R_0 at a constant small value both improves the efficiency of Monte Carlo sampling and in future work will allow GFMC calculations of correlated energy differences between states of different γ . Since the path integrals differ only at the surface, energy differences between states have smaller sampling errors than the individual energies.

Neutron-alpha scattering provides a convenient test of several important properties of low-energy nuclear scattering. There is no bound state in the $A = 5$ system, but the $3/2^-$ channel has a sharp low-energy resonance. The $1/2^-$ state is broader and higher in energy, and the combination of these two states provides a simple measure of spin-orbit splitting. Since the alpha particle is so tightly bound, simple single-channel scattering continues up to fairly high energies.

The quantity most naturally given by a GFMC calculation is the total nuclear binding, and a precision of about 1% has been the goal of past calculations. However, the quantity used to compute phase shifts is the energy relative to threshold, so a precision of 100 keV in this quantity is $\sim 0.3\%$ of the total energy in the ${}^5\text{He}$ problem. To attain this, we must choose R_0 carefully, construct a Ψ_T as close as possible to the desired GFMC solution, and use a less stringent GFMC path constraint.

First, the only *a priori* constraint on R_0 is that it should be ‘‘beyond the range’’ of the nuclear interaction. We find that our GFMC result depends on R_0 at the level of about 100 keV (out of a total of ~ -28 MeV) in going from $R_0 = 7$ to 9 fm. We find no further change going from 9 to 10 fm; the highest attainable energy (corresponding to the

state with a node at the surface) decreases as R_0 increases, so we choose $R_0 = 9$ fm.

Second, the GFMC energy also depends somewhat on the input Ψ_T . We find it important to adjust pair correlations between particles in different clusters (between the n and constituents of the α in this case) so that the factorization in Eq. (1) is enforced at large cluster separation [14]. We also adjust a parameter in Ψ_T that corresponds to k until it matches the final GFMC energy; this typically takes one or two iterations of the VMC and GFMC calculations to obtain a self-consistent result.

Finally, in all of our $A > 4$ GFMC calculations, we use a path constraint [1] on the GFMC walk to mitigate the Fermion sign problem; we compute energy samples only after releasing the constraint for some number of steps to avoid biasing the results. We find that stable results in our scattering calculations require the use of 80 unconstrained steps rather than the usual 20 to 40. However, the $\Delta\tau$ step size is unchanged.

In Fig. 1 we present phase shifts for all channels, computed with three different interaction models. In each case the AV18 potential is used as the two-nucleon interaction; in the second (third) case the UIX (IL2) three-nucleon potential is added. We also show partial-wave total cross sections for the AV18 + IL2 case in Fig. 2. Each point in these figures is equivalent in computer time to a single bound-state calculation of comparable statistical error. Because of the narrow resonance in the $3/2^-$ channel, γ

varies rapidly with E so that the highest-energy state we can reach—the first with a node at R_0 —lies lower than in the other two channels. Future calculations extending to energies beyond this maximum-energy state should be analogous to previous calculations of multiple bound states with the same quantum numbers [15].

In the figures, we compare our results with those from a multichannel R -matrix analysis of the ${}^5\text{He}$ system [16] that characterizes the measured scattering data very well ($\chi^2/\text{d.o.f.}$ is 1.6). Some of the resonance parameters from that analysis are given in Refs. [17,18]. Because there are more than 2600 data points in the analysis, the uncertainties in the R -matrix phase shifts are likely to be much smaller than the errors in the GFMC calculations.

We have made rational polynomial fits to $\tan\delta_{JL}/k^{2L+1}$, converted them to rational polynomials for the S -matrix, and used these to find the poles of S . These fits are shown as dashed curves in the figures. For each of the two p -wave states, we find just one pole that is stable as the degrees of the polynomials are changed; we identify these as the resonance poles. For $3/2^-$ the poles are at $1.19-0.77i$, $1.39-0.75i$, and $0.83-0.35i$ MeV for AV18 alone, AV18 + UIX, and AV18 + IL2, respectively, compared with $0.798-0.324i$ MeV from analysis of the data [18]. The corresponding $1/2^-$ values are $1.7-2.2i$, $2.4-2.5i$, and $2.3-2.6i$ MeV, compared with $2.07-2.79i$ MeV. The $1/2^+$ fits yield no stable pole, in agreement with the lack of a resonance in this channel and with the R -matrix analysis. All pole locations have an error of not more than 3 in the last decimal place.

It is well known that realistic two-nucleon interactions alone provide insufficient spin-orbit splitting in light nuclei

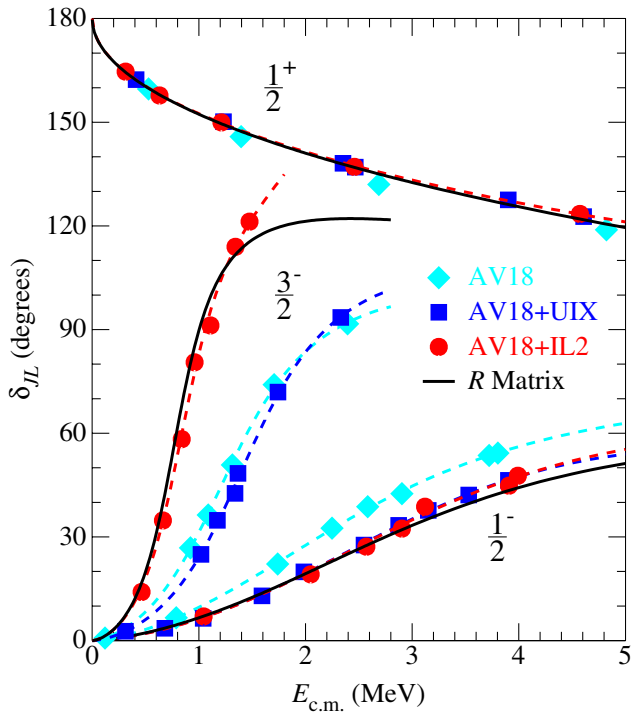


FIG. 1 (color online). Phase shifts for n - α scattering. Filled symbols (with statistical errors smaller than the symbols) are GFMC results; dashed curves are fits described in the text; and solid curves are from an R -matrix fit to data [16].

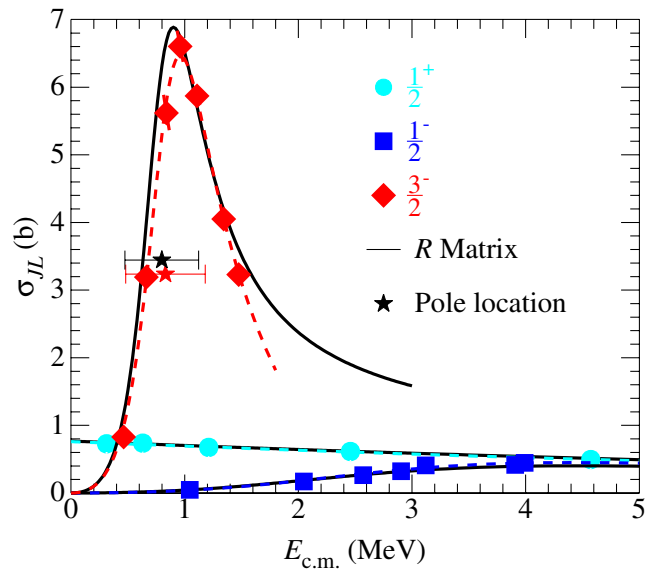


FIG. 2 (color online). Partial-wave cross sections from the AV18 + IL2 Hamiltonian compared to R -matrix analysis. Stars show the pole energies in $3/2^-$ scattering for the R -matrix fit and for AV18 + IL2, with the bars indicating the imaginary part.

[19,20]. The figures and pole positions above confirm this: the spin-orbit splitting with AV18 is less than half of what is needed to explain the data. The UIX three-nucleon potential includes a two-pion-exchange term and a phenomenological short-range repulsion, fitted simultaneously to the ^3H binding energy and the saturation density of nuclear matter. Adding UIX to AV18 increases the spin-orbit splitting, but not enough to match the data.

The IL2 potential includes the terms in the UIX model, plus a three-pion-ring exchange term and an additional two-pion-range term. The strengths of all four terms were adjusted to fit 17 energy levels in nuclei up to $A = 8$ [4]. Adding IL2 to AV18 induces even greater spin-orbit splitting in the fitted nuclei; the figures and pole positions show that the experimental ^5He splitting is almost exactly reproduced by AV18 + IL2. The widths of the resonances are also well reproduced by AV18 + IL2.

All three potentials produced essentially identical results for the $1/2^+$ case, in good agreement with data. The s -wave scattering is dominated by a node in the n - α correlation at a position that roughly fixes the zero-energy scattering length, and the wave functions for all potentials contain similar structure. All three are consistent with a scattering length of 2.4 fm, compared with an experimental scattering length of 2.46 fm [18].

We note that the energies obtained here for the resonant pole positions agree moderately well with those obtained by treating them as pseudobound states [4]: for the $3/2^-$ state we formerly had 1.6, 1.4, and 0.7 MeV for the AV18, AV18 + UIX, and AV18 + IL2, respectively, and $1/2^-$ values of 2.2, 2.5, and 2.3 MeV. However, we pointed out in Ref. [4] that there was a certain ambiguity in determining the energies of broad states because they fell slowly but steadily with imaginary time. Also, no resonance widths could be computed using pseudobound states.

In summary, we have introduced a new QMC technique to calculate low-energy scattering and applied it to neutron-alpha scattering. Models of the three-nucleon interaction that have been successful in describing bound levels of light nuclei also provide good descriptions of these scattering states. The AV18 + IL2 Hamiltonian gives a particularly good representation. The sensitivity of the results in Fig. 1 to the Hamiltonian suggests that scattering calculations can provide important additional constraints on the three-nucleon interaction.

Many extensions and applications of the computational method presented here are possible. Because these calculations are done in coordinate space, including Coulomb interactions between the clusters will pose no problems; the F_L and G_L of Eq. (1) are then simply Coulomb, rather than Bessel, functions. Extensions to nucleus-nucleus (rather than nucleon-nucleus) scattering should also be feasible. Besides pure scattering problems and the use of

scattering wave functions to compute electroweak cross sections [21] and hadronic parity violation, the scattering method should be applicable to cases with more than one open two-cluster channel. For N_{ch} such channels, a set of N_{ch} linearly independent solutions of the Schrödinger equation at the same energy determines the S matrix. The solutions could be obtained either by varying the boundary conditions at the surface, or by calculating the derivative of the energy with respect to changes in the logarithmic derivatives.

We gratefully acknowledge valuable discussions with V.R. Pandharipande. Calculations were performed on the parallel computers of the Laboratory Computing Resource Center, Argonne National Laboratory. The work of K.M.N., S.C.P., and R.B.W. is supported by the U.S. Department of Energy, Office of Nuclear Physics, under Contract No. DE-AC02-06CH11357. The work of J.C. and G.M.H. is supported by the U.S. Department of Energy under Contract No. DE-AC52-06NA25396.

-
- [1] R. B. Wiringa *et al.*, Phys. Rev. C **62**, 014001 (2000).
 - [2] S. C. Pieper, K. Varga, and R. B. Wiringa, Phys. Rev. C **66**, 044310 (2002).
 - [3] P. Navrátil and W. E. Ormand, Phys. Rev. C **68**, 034305 (2003).
 - [4] S. C. Pieper *et al.*, Phys. Rev. C **64**, 014001 (2001).
 - [5] J. Carlson, V. R. Pandharipande, and R. B. Wiringa, Nucl. Phys. A **424**, 47 (1984).
 - [6] J. Carlson, K. E. Schmidt, and M. H. Kalos, Phys. Rev. C **36**, 27 (1987).
 - [7] J. Carlson, Nucl. Phys. A **522**, 185c (1991).
 - [8] R. B. Wiringa, V. G. J. Stoks, and R. Schiavilla, Phys. Rev. C **51**, 38 (1995).
 - [9] B. S. Pudliner *et al.*, Phys. Rev. Lett. **74**, 4396 (1995).
 - [10] Y. Alhassid and S. E. Koonin, Ann. Phys. (N.Y.) **155**, 108 (1984).
 - [11] B. S. Pudliner *et al.*, Phys. Rev. C **56**, 1720 (1997).
 - [12] J. Shumway and D. M. Ceperley, Phys. Rev. B **63**, 165209 (2001).
 - [13] S. Chiesa, M. Mella, and G. Morosi, Phys. Rev. A **66**, 042502 (2002); **69**, 022701 (2004).
 - [14] K. M. Nollett, R. B. Wiringa, and R. Schiavilla, Phys. Rev. C **63**, 024003 (2001).
 - [15] S. C. Pieper, R. B. Wiringa, and J. Carlson, Phys. Rev. C **70**, 054325 (2004).
 - [16] G. M. Hale, D. C. Dodder, and K. Witte (unpublished).
 - [17] A. Csótó and G. M. Hale, Phys. Rev. C **55**, 536 (1997).
 - [18] D. R. Tilley *et al.*, Nucl. Phys. A **708**, 3 (2002).
 - [19] S. C. Pieper and V. R. Pandharipande, Phys. Rev. Lett. **70**, 2541 (1993).
 - [20] J. Fujita and H. Miyazawa, Prog. Theor. Phys. **17**, 360 (1957); **17**, 366 (1957).
 - [21] L. E. Marcucci *et al.*, Nucl. Phys. A **777**, 111 (2006).